Width-induced metal insulator transition in SrVO3 lateral nanowires spontaneously formed on the ultrathin film

Applied Physics Letters

Width-induced metal–insulator transition in $SrVO_3$ lateral nanowires spontaneously formed on the ultrathin film

Cite as: Appl. Phys. Lett. **117**, 051603 (2020); https://doi.org/10.1063/5.0018240
Submitted: 12 June 2020 . Accepted: 24 July 2020 . Published Online: 06 August 2020

Hirofumi Oka, Yoshinori Okada, Kenichi Kaminaga, Daichi Oka, Taro Hitosugi, and Tomoteru Fukumura

Applied Physics Letters ARTICLE scitation.org/journal/apl

Width-induced metal–insulator transition in $SrVO_3$ lateral nanowires spontaneously formed on the ultrathin film

Cite as: Appl. Phys. Lett. **117**, 051603 (2020); doi: 10.1063/5.0018240
Submitted: 12 June 2020 · Accepted: 24 July 2020 ·
Published Online: 6 August 2020

Hirofumi Oka,[1,2,a)] Yoshinori Okada,[1,3] Kenichi Kaminaga,[1] Daichi Oka,[4] Taro Hitosugi,[1,5] and Tomoteru Fukumura[1,2,4]

AFFILIATIONS

[1]Advanced Institute for Materials Research, Tohoku University, Sendai 980-8577, Japan
[2]Core Research Cluster, Tohoku University, Sendai 980-8577, Japan
[3]Okinawa Institute of Science and Technology Graduate University, Okinawa 904-0495, Japan
[4]Department of Chemistry, Graduate School of Science, Tohoku University, Sendai 980-8578, Japan
[5]Department of Chemical Science and Engineering, School of Materials and Chemical Technology, Tokyo Institute of Technology, Tokyo 152-8550, Japan

[a)]**Author to whom correspondence should be addressed:** hirofumi.oka.e3@tohoku.ac.jp

ABSTRACT

We investigated lateral nanowires at the topmost layer of $SrVO_3$ (001) ultrathin films using *in situ* low-temperature scanning tunneling microscopy and spectroscopy. The nanowires were spontaneously formed in the topmost layer of $SrVO_3$ with a $(\sqrt{2} \times \sqrt{2})$-*R*45° reconstruction on the terrace of a $(\sqrt{5} \times \sqrt{5})$-*R*26.6° reconstruction. The electronic states of nanowires were significantly influenced by the nanowire width. With reducing the nanowire width from 5.5 nm to 1.7 nm, the zero-bias conductance of nanowires steeply decreased toward zero, exhibiting a metal–insulator transition possibly driven by dimensional crossover, previously observed in thickness-reduced $SrVO_3$ ultrathin films.

Strongly correlated transition metal oxides (TMOs) show intriguing quantum phenomena such as high temperature superconductivity, colossal magnetoresistance, and metal–insulator transition, driven by interplay between charge, spin, and orbital degrees of freedom.[1] Reduced dimensionality of TMOs further provides emergent properties, for example, a high-mobility two-dimensional electron gas and a superconducting phase at the $LaAlO_3/SrTiO_3$ interface[2,3] and metal–insulator transition in various TMO ultrathin films and superlattices.[4–10] As for one-dimensional structures, 2-nm-wide conducting channels of the $LaAlO_3/SrTiO_3$ interface have been achieved by top-down atomic force microscope lithography to exhibit quantized ballistic transport.[11,12] Also, sub-micrometer-wide VO_2 wires were fabricated with a nanoimprint lithography to resolve a phase separation composed of tens of nanometers-wide metallic and insulating domains.[13,14] So far, a nanometer-wide local structure of TMOs has not been realized by the bottom-up approach. In addition, it is intriguing to observe electronic states of one-dimensional TMOs because one-dimensional effects on the band structure of TMOs have not been investigated experimentally.

To explore the electronic correlation in low-dimensional TMO systems, a perovskite-type $SrVO_3$ has been extensively investigated because of its simple cubic symmetry and $3d^1$ electronic configuration. In $SrVO_3$ ultrathin films, two-dimensional quantum well states have been formed due to the confinement of correlated electrons,[15–18] and the metal–insulator transition has been driven by dimensional crossover.[6,9,19] Until now, one-dimensional structures of $SrVO_3$ such as nanowires have not been investigated.

In this paper, we report spontaneous formation of one-dimensional $SrVO_3$ nanowires in the topmost layer of $SrVO_3$ ultrathin films. The electronic states of $SrVO_3$ ultrathin films as a function of the nanowire width were investigated by using low-temperature scanning tunneling microscopy and spectroscopy (STM and STS). The electronic states of the nanowires were strongly influenced by the nanowire width, varying from metallic to insulating with decreasing the nanowire width. This

result is reminiscent of the metal–insulator transition observed in thickness-reduced $SrVO_3$ ultrathin films,[6,9,19,20] implying a nanoscale metal–insulator transition in $SrVO_3$ nanowires.

$SrVO_3$ (001) ultrathin films were epitaxially grown on Nb (0.05 wt. %)-doped $SrTiO_3$ (001) substrates (Shinkosha Co., Ltd.) by using pulsed laser deposition with a base pressure of 5×10^{-10} Torr. Prior to thin film growth, the substrates were heated at 500 °C for 30 min followed by annealing at 1000 °C for 1 h under an oxygen partial pressure of 1×10^{-6} Torr. A $Sr_2V_2O_7$ polycrystalline target (Kojundo Chemical Laboratory Co., Ltd.) was ablated by a KrF excimer laser ($\lambda = 248$ nm) with a pulse frequency of 2 Hz and a laser fluence of 1 J/cm^2. The ultrathin film was deposited at 850 °C under ultrahigh vacuum (UHV) with a deposition rate of 0.01 unit cell (UC) per pulse, which was determined by reflection high energy electron diffraction intensity oscillations during film deposition.[21] The film thickness was 8 UC, approximately 3 nm thick. After deposition, the samples were cooled down to room temperature and then *in situ* transferred to a pre-cooled STM head without breaking UHV.[22,23] STM and STS measurements were performed with electrochemically etched W tips at 78 K. All STS measurements were performed with an open feedback loop. The setpoints of voltage and current (V_{stab} and I_{stab}, respectively) to stabilize the tip before opening feedback loop are indicated in figure captions.

Figure 1(a) shows an STM image of the $SrVO_3$ ultrathin film on the $SrTiO_3$ (001) substrate. The STM image revealed one-dimensional nanowire structures formed on atomically flat terraces, indicated by white arrows in Fig. 1(a). In addition, most of the nanowires were found to terminate at corners of terraces as shown by dashed circles, indicating that the corners became nucleation sites of the nanowires. Figure 1(b) shows a height profile along a red arrow in Fig. 1(a). The width of nanowires evaluated by the full width at half maximum of their heights was 2.76 nm, 2.76 nm, and 1.78 nm from the left to right in Fig. 1(b), approximately corresponding to 7.3, 7.3, and 4.7 UC, respectively. The height of the nanowires was about 0.2 nm, corresponding to a half UC of $SrVO_3$, 0.38 nm.

Atomically resolved STM images of the $SrVO_3$ nanowires were observed. Figures 2(a) and 2(b) show large-area and high-resolution STM images of the $SrVO_3$ ultrathin film, respectively, where the blue squared area in Fig. 2(a) corresponds to Fig. 2(b). As seen in Fig. 2(b), the nanowire at the bottom side possessed the same square lattice

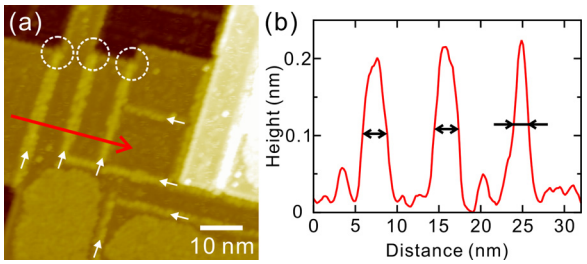

FIG. 1. (a) STM image of the $SrVO_3$ (001) ultrathin film on the $SrTiO_3$ (001) substrate (sample bias voltage $V = -1.0$ V, tunneling current $I = 10$ pA, and scanned area 60×60 nm^2). The white arrows indicate nanowires on atomically flat terraces. The white dashed circles denote terminations of the nanowires at corners of terraces. (b) Height profile along the red arrow in (a). The black arrows denote the full widths of nanowires at half maximum of their heights.

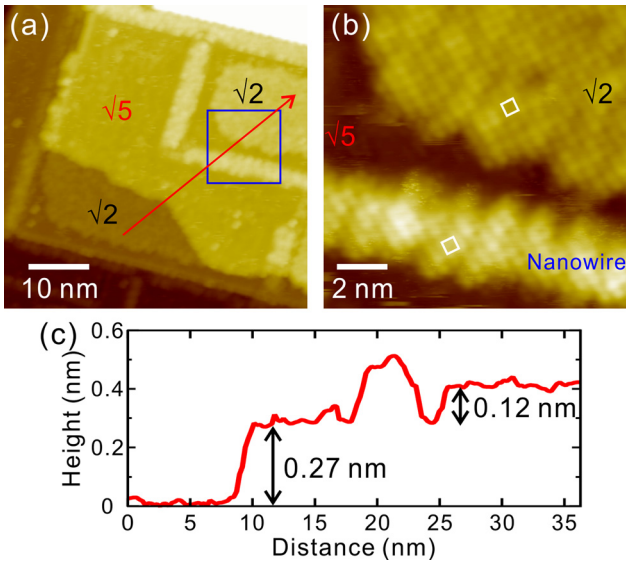

FIG. 2. (a) STM image of the $SrVO_3$ (001) ultrathin film ($V = -1.0$ V, $I = 10$ pA, and 50×50 nm^2). Terraces with ($\sqrt{2} \times \sqrt{2}$)-*R*45° and ($\sqrt{5} \times \sqrt{5}$)-*R*26.6° structures are labeled as $\sqrt{2}$ and $\sqrt{5}$, respectively. (b) Atomic-resolution STM image of the area at the blue square in (a) ($V = -0.5$ V, $I = 20$ pA, and 12×12 nm^2). The white squares indicate unit cells of a ($\sqrt{2} \times \sqrt{2}$)-*R*45° structure. (c) Height profile along the red arrow in (a).

structure with a periodicity of 0.54 nm as an adjacent flat terrace at the upper side (indicated as white squares), corresponding to a ($\sqrt{2} \times \sqrt{2}$)-*R*45° reconstruction of apical oxygen atoms as was reported previously.[21,24,25] Figure 2(c) shows a height profile along a red arrow in Fig. 2(a), representing that the terraces had two different step heights, 0.27 nm and 0.12 nm, where the nanowire was formed on the former terrace. Since $SrVO_3$ ultrathin films on $SrTiO_3$ had two-surface reconstructions with different step heights, 0.22 nm for ($\sqrt{5} \times \sqrt{5}$)-*R*26.6° and 0.16 nm for ($\sqrt{2} \times \sqrt{2}$)-*R*45°,[25] the nanowire was formed on the ($\sqrt{5} \times \sqrt{5}$)-*R*26.6° terrace. The taller nanowire than the ($\sqrt{2} \times \sqrt{2}$)-*R*45° terrace with the step height of 0.12 nm in spite of the same atomic structure was attributed to different electronic states as described below.

Figure 3(a) shows differential conductance (d*I*/d*V*) spectra measured on a nanowire and ($\sqrt{2} \times \sqrt{2}$)-*R*45° and ($\sqrt{5} \times \sqrt{5}$)-*R*26.6° terraces, where the d*I*/d*V* signal with STS is proportional to the local density of states of the sample.[26] The differential conductance larger for the nanowire than that for the ($\sqrt{2} \times \sqrt{2}$)-*R*45° terrace at $V = -1.0$ V resulted in an apparently taller nanowire than the ($\sqrt{2} \times \sqrt{2}$)-*R*45° terrace in Fig. 2(c) since all STM images were acquired in the constant current mode. The large differential conductance at $V = 0$ V [zero-bias conductance (ZBC)] of ($\sqrt{2} \times \sqrt{2}$)-*R*45° terrace while the strongly reduced ZBC of ($\sqrt{5} \times \sqrt{5}$)-*R*26.6° terrace were observed, being consistent with the previous study.[25] Interestingly, the ZBC was further reduced for the nanowire [Fig. 3(a)].

To visualize spatial distribution of the ZBC, STS measurements were performed at the area of an STM image indicated in Fig. 3(b). Figure 3(c) shows a d*I*/d*V* map at $V = 0$ V, i.e., a ZBC map. Large and medium ZBC areas, corresponding to ($\sqrt{2} \times \sqrt{2}$)-*R*45° and ($\sqrt{5} \times \sqrt{5}$)-*R*26.6° terraces, respectively, were roughly partitioned by 2–3 nm wide

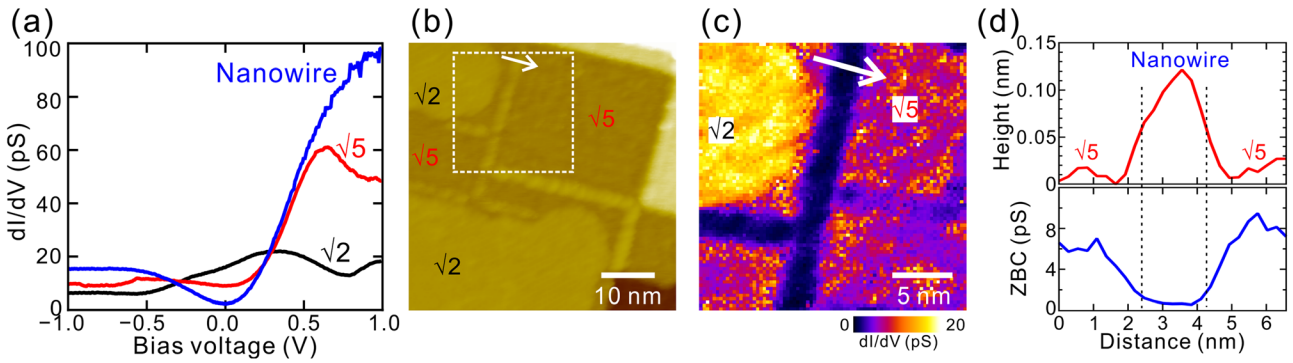

FIG. 3. (a) Differential conductance (dI/dV) spectra of a nanowire and ($\sqrt{2} \times \sqrt{2}$)-*R*45° and ($\sqrt{5} \times \sqrt{5}$)-*R*26.6° terraces on the $SrVO_3$ (001) ultrathin film ($V_{stab} = 0.5$ V and $I_{stab} = 10$ pA). (b) STM image of the $SrVO_3$ (001) ultrathin film ($V = 0.5$ V, $I = 10$ pA, and 50×50 nm^2). The ($\sqrt{2} \times \sqrt{2}$)-*R*45° and ($\sqrt{5} \times \sqrt{5}$)-*R*26.6° terraces are labeled as $\sqrt{2}$ and $\sqrt{5}$, respectively. (c) ZBC map of the area at the white dashed square in (b) ($V_{stab} = 0.5$ V, $I_{stab} = 10$ pA, and 22×22 nm^2). (d) The height (upper panel) and the ZBC (lower panel) profiles across a nanowire along the white arrows in (b) and (c), respectively. The dashed lines indicate the positions at a half height of the nanowire.

nanowires with approximately zero ZBC, indicating that the nanowires were electronically separated from their surrounding terraces. Figure 3(d) shows the height (upper panel) and the ZBC (lower panel) profiles across a nanowire between ($\sqrt{5} \times \sqrt{5}$)-*R*26.6° terraces [white arrows in Figs. 3(b) and 3(c), respectively]. The ZBC of the nanowire was as small as 1 pS. These results represent that electronic states of the $SrVO_3$ ultrathin film surface are governed by not only the surface reconstructions but also the one-dimensional confinement.

Figure 4 shows ZBC of nanowires as a function of the nanowire width. The ZBC was almost constant and very close to that of the ($\sqrt{2} \times \sqrt{2}$)-*R*45° terrace for the nanowire width down to 5.5 nm. However, the ZBC steeply decreased with narrowing the width down to 1.7 nm, being significantly smaller than that of the ($\sqrt{5} \times \sqrt{5}$)-*R*26.6° terrace, corresponding to an insulating state. This result represents that the ZBC was strongly influenced by the nanowire width.

TMO thin films and superlattices have been reported to undergo metal–insulator transition with decreasing their thicknesses.[4–10,20] According to photoemission spectroscopy of $SrVO_3$ ultrathin films by Yoshimatsu *et al.*, the photoemission-intensity at E_F showed metallic nature for 6 UC thickness, but decreased to zero below 3 UC thickness.[6] From dynamical mean-field theory calculations, the thickness-dependent photoemission-intensity at E_F was attributed to metal–insulator transition caused by the bandwidth reduction due to dimensional crossover.[6] As seen from Fig. 4, the ZBC rapidly decreased toward zero for the nanowires with 6 UC wide or less. This tendency was quite similar to the results of Yoshimatsu *et al.*,[6] implying a similar mechanism of the metal–insulator transition for the thickness-reduced $SrVO_3$ ultrathin films and the width-reduced $SrVO_3$ nanowires.

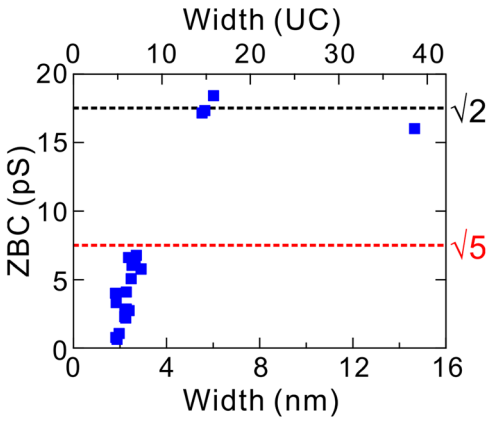

FIG. 4. Zero-bias conductance (ZBC) of nanowires on the $SrVO_3$ (001) ultrathin film as a function of the nanowire width in units of nm and UC, where 1 UC corresponds to 0.38 nm. The black and red dashed lines denote averaged ZBCs of ($\sqrt{2} \times \sqrt{2}$)-*R*45° and ($\sqrt{5} \times \sqrt{5}$)-*R*26.6° terraces, respectively ($V_{stab} = 0.5$ V and $I_{stab} = 10$ pA).

In conclusion, we formed $SrVO_3$ nanowires spontaneously on the ultrathin film and investigated the influence of the nanowire width on the electronic states using low-temperature STM/STS. We found that the ZBC of nanowires significantly decreased with narrowing nanowires, possibly attributed to a metal–insulator transition driven by dimensional crossover, similar to the metal–insulator transition in thickness-reduced $SrVO_3$ ultrathin films.[6]

This study was supported by JSPS KAKENHI (Nos. 17H02779, 18H03876, 18K18935, and 20H04624).

DATA AVAILABILITY

The data that support the findings of this study are available from the corresponding author upon reasonable request.

REFERENCES

[1]Y. Tokura and N. Nagaosa, Science **288**, 462 (2000).
[2]A. Ohtomo and H. Y. Hwang, Nature **427**, 423 (2004).
[3]N. Reyren, S. Thiel, A. D. Caviglia, L. F. Kourkoutis, G. Hammerl, C. Richter, C. W. Schneider, T. Kopp, A.-S. Rüetschi, D. Jaccard, M. Gabay, D. A. Muller, J.-M. Triscone, and J. Mannhart, Science **317**, 1196 (2007).
[4]J. Xia, W. Siemons, G. Koster, M. R. Beasley, and A. Kapitulnik, Phys. Rev. B **79**, 140407 (2009).
[5]J. Son, P. Moetakef, J. M. LeBeau, D. Ouellette, L. Balents, S. J. Allen, and S. Stemmer, Appl. Phys. Lett. **96**, 062114 (2010).
[6]K. Yoshimatsu, T. Okabe, H. Kumigashira, S. Okamoto, S. Aizaki, A. Fujimori, and M. Oshima, Phys. Rev. Lett. **104**, 147601 (2010).
[7]A. V. Boris, Y. Matiks, E. Benckiser, A. Frano, P. Popovich, V. Hinkov, P. Wochner, M. Castro-Colin, E. Detemple, V. K. Malik, C. Bernhard, T. Prokscha, A. Suter, Z. Salman, E. Morenzoni, G. Cristiani, H. U. Habermeier, and B. Keimer, Science **332**, 937 (2011).

[8]R. Scherwitzl, S. Gariglio, M. Gabay, P. Zubko, M. Gibert, and J.-M. Triscone, Phys. Rev. Lett. **106**, 246403 (2011).
[9]A. Fouchet, M. Allain, B. Bérini, E. Popova, P.-E. Janolin, N. Guiblin, E. Chikoidze, J. Scola, D. Hrabovsky, Y. Dumont, and N. Keller, Mater. Sci. Eng. B **212**, 7 (2016).
[10]P. Schütz, D. Di Sante, L. Dudy, J. Gabel, M. Stübinger, M. Kamp, Y. Huang, M. Capone, M.-A. Husanu, V. N. Strocov, G. Sangiovanni, M. Sing, and R. Claessen, Phys. Rev. Lett. **119**, 256404 (2017).
[11]M. Tomczyk, G. Cheng, H. Lee, S. Lu, A. Annadi, J. P. Veazey, M. Huang, P. Irvin, S. Ryu, C.-B. Eom, and J. Levy, Phys. Rev. Lett. **117**, 096801 (2016).
[12]A. Annadi, G. Cheng, H. Lee, J.-W. Lee, S. Lu, A. Tylan-Tyler, M. Briggeman, M. Tomczyk, M. Huang, D. Pekker, C.-B. Eom, P. Irvin, and J. Levy, Nano Lett. **18**, 4473 (2018).
[13]H. Takami, K. Kawatani, H. Ueda, K. Fujiwara, T. Kanki, and H. Tanaka, Appl. Phys. Lett. **101**, 263111 (2012).
[14]Y. Tsuji, T. Kanki, Y. Murakami, and H. Tanaka, Appl. Phys. Express **12**, 025003 (2019).
[15]K. Yoshimatsu, K. Horiba, H. Kumigashira, T. Yoshida, A. Fujimori, and M. Oshima, Science **333**, 319 (2011).
[16]K. Yoshimatsu, E. Sakai, M. Kobayashi, K. Horiba, T. Yoshida, A. Fujimori, M. Oshima, and H. Kumigashira, Phys. Rev. B **88**, 115308 (2013).
[17]M. Kobayashi, K. Yoshimatsu, E. Sakai, M. Kitamura, K. Horiba, A. Fujimori, and H. Kumigashira, Phys. Rev. Lett. **115**, 76801 (2015).
[18]M. Kobayashi, K. Yoshimatsu, T. Mitsuhashi, M. Kitamura, E. Sakai, R. Yukawa, M. Minohara, A. Fujimori, K. Horiba, and H. Kumigashira, Sci. Rep. **7**, 16621 (2017).
[19]M. Gu, S. A. Wolf, and J. Lu, Adv. Mater. Interfaces **1**, 1300126 (2014).
[20]G. Wang, Z. Wang, M. Meng, M. Saghayezhian, L. Chen, C. Chen, H. Guo, Y. Zhu, E. W. Plummer, and J. Zhang, Phys. Rev. B **100**, 155114 (2019).
[21]Y. Okada, S.-Y. Shiau, T.-R. Chang, G. Chang, M. Kobayashi, R. Shimizu, H.-T. Jeng, S. Shiraki, H. Kumigashira, A. Bansil, H. Lin, and T. Hitosugi, Phys. Rev. Lett. **119**, 86801 (2017).
[22]K. Iwaya, R. Shimizu, T. Hashizume, and T. Hitosugi, Rev. Sci. Instrum. **82**, 083702 (2011).
[23]K. Iwaya, T. Ohsawa, R. Shimizu, Y. Okada, and T. Hitosugi, Sci. Technol. Adv. Mater. **19**, 282 (2018).
[24]K. Fuchigami, Z. Gai, T. Z. Ward, L. F. Yin, P. C. Snijders, E. W. Plummer, and J. Shen, Phys. Rev. Lett. **102**, 66104 (2009).
[25]H. Oka, Y. Okada, T. Hitosugi, and T. Fukumura, Appl. Phys. Lett. **113**, 171601 (2018).
[26]H. Oka, O. O. Brovko, M. Corbetta, V. S. Stepanyuk, D. Sander, and J. Kirschner, Rev. Mod. Phys. **86**, 1127 (2014).